Spectrum Sensing for Cognitive Radio Based on Multiple Antennas

Nguyen, Huan Cong; De Carvalho, Elisabeth; Prasad, Ramjee

Published in:
2012 IEEE 75th Vehicular Technology Conference (VTC Spring)

DOI (link to publication from Publisher):
10.1109/VETECS.2012.6239985

Publication date:
2012

Document Version
Publisher's PDF, also known as Version of record

Spectrum Sensing for Cognitive Radio Based on Multiple Antennas

Huan Cong Nguyen, Elisabeth de Carvalho and Ramjee Prasad
Department of Electronic Systems, Faculty of Engineering and Science,
Aalborg University, DK-9220 Aalborg, Denmark
Email: {hcn|edc|prasad}@es.aau.dk

***Abstract*—Spectrum sensing is a key component for enabling the cognitive radio paradigm. In this paper, we propose a novel totally-blind spectrum sensing technique for cognitive radio device equipped with multiple antennas, namely the Space Frequency Cross Product Sensing (SFCPS) algorithm. Existing correlation-based spectrum sensing techniques rely on the assumption that the received signals are correlated and their performance becomes poor when the signal correlation is low. By appropriately combining the received signals from multiple antennas, the proposed method creates new signals that are fully correlated and on which a sensing method is developed. SFCPS performs better than existing correlation-based techniques and with a lower computational complexity for small number of observed samples.**

***Index Terms*—spectrum sensing, signal detection, multiple antennas, antenna arrays, cognitive radio, signal processing, blind detection.**

I. Introduction

The spectrum scarcity has led to the abandonment of traditional models of radio frequency (RF) management, opening up portions of the licensed spectrum for cognitive radio devices. Cognitive radio, a relatively new paradigm for wireless communication, allows a secondary user to opportunistically and dynamically utilize the unused RF bands, which are assigned to a primary user. A key component of cognitive radio is spectrum sensing, where the secondary user monitors the spectrum and identifies idle bands for its own communication.

In [1], non-cooperative spectrum sensing is categorized into three different groups: 1) methods requiring information about some part of the source signal (e.g. training sequence or pilots) and about the noise power, 2) methods requiring only noise power information (semiblind detection), and 3) methods requiring no information on source signal or noise power (totally blind detection). The first group consists of the likelihood ratio test (LRT) [2], matched-filter (MF) detection [2] and cyclostationary feature (CSF) detection [3], while examples of the second category include the energy detection (ED) [4], [5] and wavelet-based sensing [6]. The third group, which is the focus of this paper, consists of the covariance-based sensing [7] and eigenvalue-based sensing [8], [9]. Those methods exploit the correlation in the received signal in the time domain, due to the time dispersion of the channel, oversampling or inherent correlation property of the signal. They are applicable for both single- and multiple receive antenna cases where the signal correlation across antennas can be additionally exploited. Their performance depends on both the correlation strength among the signal samples and the size of observation: if the correlation strength is low, the number of observed samples must be increased to compensate for the weak correlation. Otherwise, there exists an upper limit on the probability of detection even in noise-free environment, a phenomena we refer to as the *ceiling effect*.

In this paper, we propose a frequency domain sensing technique applicable to frequency selective channels and receivers equipped with multiple antennas, which will be a common feature for wireless devices in the future. Based on a cross product of the received signals in space and frequency, we create new signals that are fully correlated and develop a sensing technique exploiting those new fully correlated signals. We call this technique Space Frequency Cross Product Sensing (SFCPS):

- SFCPS outperforms the existing correlation-based methods, especially for a small number of observed samples. Because SFCPS is based on fully-correlated signals, it does not experience the ceiling effect. It can achieve 100% probability of detection at $SNR > 0$ for relatively small observation size.
- The threshold in SFCPS does not depend on observation size, and it can be conveniently computed from the target probability of false alarm.

The rest of the paper is organized as follows: the system model and the SFCPS algorithm are presented in Section II. Section III finds the thresholds and provides the performance analysis. We discuss the simulation results in Section IV. Finally, conclusions and future works are summarized in Section V. Here are notation used throughout this paper: boldface letters denote matrices and vectors, the $\odot$ represents Schur product (i.e. the elementwise product of two matrices of the same dimensions), and the superscripts *, T and H stand for complex conjugate, transpose and Hermitian (transpose-conjugate), respectively. The $\lfloor . \rfloor_N$ is modulo-N operator.

II. Space Frequency Cross Product Sensing

Consider a primary transmitter sending one data stream (e.g. using a beamforming technique) and a secondary receiver with $\mathcal{Q} \geq 2$ antennas. There are two hypotheses: $\mathcal{H}_0$, the primary transmitter is transmitting, and $\mathcal{H}_1$, the primary transmitter is not transmitting. The continuous-time baseband received signal at the q^{th} antenna is given by:

978-1-4673-0990-5/12/$31.00 ©2012 IEEE

$$\mathcal{H}_0 : \tilde{y}_q(t) = \tilde{w}_q(t) \tag{1}$$
$$\mathcal{H}_1 : \tilde{y}_q(t) = \tilde{z}_q(t) + \tilde{w}_q(t) \qquad q = 1, 2, \ldots \mathcal{Q}$$

where $\tilde{y}_q(t)$, $\tilde{z}_q(t)$ and $\tilde{w}_q(t)$ is the continuous-time received signal, the received source signal and the Additive White Gaussian Noise (AWGN) at the q^{th} antenna of the secondary receiver, respectively. The received source signal $\tilde{z}_q(t)$ contains the effect of the frequency-selective channel, which is assumed to be time-invariant during the observation period:

$$\tilde{z}_q(t) = \sum_{l=1}^{\mathcal{L}} h_q(l)\tilde{x}(t - \tau_l) \tag{2}$$

where $h_q(l)$ and τ_l are the complex channel gain and time delay of the l^{th} multipath component at the q^{th} receive antenna, respectively. And $\tilde{x}(t)$ is the transmitted symbol from the primary transmitter.

A. Space-frequency cross product

The data is processed by blocks: a Discrete Fourier Transform (DFT) is performed over each block allowing for a sensing technique in the frequency domain. Consider the b^{th} block of the received source signal corresponding to observation period of T_o:

$$\begin{aligned}\tilde{z}_{qb}(t) &\triangleq \tilde{z}_q(t)\Xi_{T_o}(t - bT_o) \\ &= \sum_{l=1}^{\mathcal{L}} h_q(l)\tilde{x}(t - \tau_l)\Xi_{T_o - \tau_{max}}(t - bT_o - \tau_l) \\ &+ \sum_{l=1}^{\mathcal{L}} h_q(l)\tilde{x}(t - \tau_l)\Xi_{\tau_l}(t - bT_o) \\ &+ \sum_{l=1}^{\mathcal{L}} h_q(l)\tilde{x}(t - \tau_l)\Xi_{\tau_{max} - \tau_l}(t - (b+1)T_o - \tau_l)\end{aligned} \tag{3}$$

in which $\tau_{max} = \text{argmax}_l(\tau_l)$ is the maximum time delay of the channel impulse response (CIR) and $\Xi_T(t)$ denotes the unity amplitude gate pulse of length T. The first term in Eq. (3) is the useful part for our algorithm, which is the convolution of the transmitted signal $\tilde{x}_b(t) \triangleq \tilde{x}(t)\Xi_{T_o - \tau_{max}}(t - bT_o)$ with the frequency-selective fading channel. Because the channel has a delay spreading more than one symbol duration, block b contains contributions from the previous and next block: the second and the third terms in Eq. (3) indicates those two residual parts. Assume that $T_o \gg \tau_{max}$, and the energy of $\tilde{x}(t)$ is distributed evenly over time, we can neglect the effect of the residuals and consider the following approximation:

$$\tilde{z}_{qb}(t) \approx \sum_{l=1}^{\mathcal{L}} h_q(l)\tilde{x}_b(t - \tau_l) \tag{4}$$

Assume that the primary transmission is band-limited with bandwidth of $2B$, and the received signal is sampled at rate $f_s \geq 2B$. The samples are stacked into blocks of size N, and for notation simplicity, we define $\mathbf{y}_{qb} \triangleq \left[\tilde{y}_{qb}(0)\ \tilde{y}_{qb}(1) \ldots\ \tilde{y}_{qb}(N-1)\right]^T$, $\mathbf{z}_{qb} \triangleq \left[\tilde{z}_{qb}(0)\ \tilde{z}_{qb}(1) \ldots\ \tilde{z}_{qb}(N-1)\right]^T$ and $\mathbf{w}_{qb} \triangleq \left[\tilde{w}_{qb}(0)\ \tilde{w}_{qb}(1) \ldots\ \tilde{w}_{qb}(N-1)\right]^T$, where $\tilde{y}_{qb}(n) \triangleq \tilde{y}_q\big((n + bN)T\big)$, $\tilde{z}_{qb}(n) \triangleq \tilde{z}_q\big((n + bN)T\big)$ and $\tilde{w}_{qb}(n) \triangleq \tilde{w}_q\big((n + bN)T\big)$, for the b^{th} block. The DFT of $\mathbf{y}_{qb}$, $\mathbf{z}_{qb}$ and $\mathbf{w}_{qb}$ are denoted as $\mathbf{Y}_{qb} \triangleq [Y_{qb}(0)\ Y_{qb}(1) \ldots\ Y_{qb}(N-1)]^T$, $\mathbf{Z}_{qb} \triangleq [Z_{qb}(0)\ Z_{qb}(1) \ldots\ Z_{qb}(N-1)]^T$ and $\mathbf{W}_{qb} \triangleq [W_{qb}(0)\, W_{qb}(1) \ldots W_{qb}(N-1)]^T$, respectively. We can show that the k^{th} element of $\mathbf{Z}_{qb}$ is as follows:

$$Z_{qb}(k) = H_q(k)X_b(k) \tag{5}$$

in which $H_q(k) \triangleq \tilde{H}_q(\frac{2\pi k}{N})$ and $X_b(k) \triangleq \tilde{X}_b(\frac{2\pi k}{N})$, where $\tilde{H}_q(\omega)$ and $\tilde{X}_b(\omega)$ are the Fourier transforms of $h_q(l)$ and $\tilde{x}_b(t)$ after sampling, respectively [10]. The Eq. (5) indicates that the DFT of the discrete-time received source signal is proportional to the product of the spectrum of transmitted signal and the CIR.

Without loss of generality, we consider two consecutive blocks ($b = 1, 2$). Furthermore, we consider only two received antennas. The proposed scheme can be extended to more antennas by considering all the possible antenna pairs: the details of this case will be the object of future publications. The signal at antenna 1 and antenna 2 are:

$$Z_{11}(k) = H_1(k)X_1(k) \qquad Z_{12}(k) = H_1(k)X_2(k) \tag{6}$$
$$Z_{21}(k) = H_2(k)X_1(k) \qquad Z_{22}(k) = H_2(k)X_2(k) \tag{7}$$

Forming the cross-products, we observe the following relationship for all k:

$$Z_{11}(k)Z_{22}(k) = Z_{21}(k)Z_{12}(k) \tag{8}$$

Denoting the cross-products of the received signals as:

$$V_1(k) = Y_{11}(k)Y_{22}(k) \quad \text{and} \quad V_2(k) = Y_{21}(k)Y_{12}(k) \tag{9}$$

From Eq. (8), there exists a strong correlation between the two signal sequences $\{V_1(k)\}$ and $\{V_2(k)\}$ when receiving a signal from the primary transmitter. On the other hand, the correlation is zero when there is only noise in the received signal. Based on this property, we propose the following spectrum sensing method.

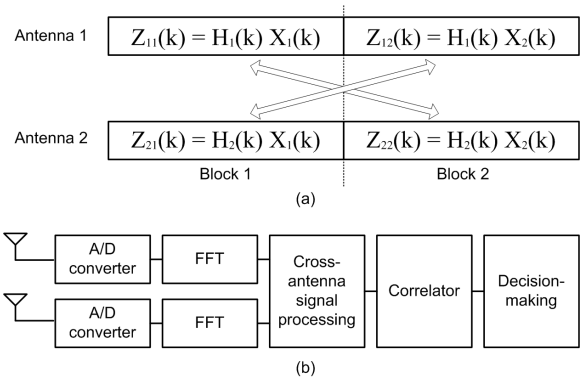

Fig. 1. (a) The space-frequency cross-product signal processing, and (b) the block diagram of the SFCPS algorithm.

B. Proposed Algorithm for Spectrum Sensing

The Space Frequency Cross Product Sensing Algorithm

Step 1: Sample the received signals from the two antennas and perform the DFT to obtain $Y_{11}(k)$, $Y_{12}(k)$, $Y_{21}(k)$ and $Y_{22}(k)$ for all k, as described in section II-A. Compute the cross-products $V_1(k)$ and $V_2(k)$ for all k according to Eq. (9).

Step 2: Calculate the coefficients of the circular correlation of $\{V_1(k)\}$ and $\{V_2(k)\}$:

$$\lambda(i) \triangleq \frac{1}{N}\sum_{k=0}^{N-1} V_1(k)V_1\big(\lfloor k-i \rfloor_N\big)^* \tag{10}$$

Step 3: Compute these two variables from the correlation:

$$T_1 \triangleq |\lambda(0)| \qquad T_2 \triangleq \frac{1}{N-1}\sum_{i=1}^{N-1}|\lambda(i)| \tag{11}$$

Step 4: Determine the presence of the signal based on T_1, T_2 and a predetermined threshold γ: If $T_1/T_2 > \gamma$, the spectrum is occupied by the primary system; otherwise, the spectrum is available.

Remark: The circular cross-correlation is chosen in step 2 to ease the computational complexity, as it can be computed efficiently by the mean of Fast Fourier Transform (FFT).

III. Threshold And Performance Analysis

The performance of our signal detection algorithm is measured by the probability of detection $\mathrm{P_d}$ and the probability of false alarm $\mathrm{P_{fa}}$. The choice of threshold γ is a trade-off between $\mathrm{P_{fa}}$ and $\mathrm{P_d}$: a large threshold reduces the chance of false alarm, but also decreases the chance of successful detection. The threshold value is derived from a target $\mathrm{P_{fa}}$, since we do not have information about the signal [7]. Once the threshold is fixed, we can compute the corresponding $\mathrm{P_d}$.

We assume that the transmitted signal, $X_b(k)$, and the channel, $H_q(k)$, are independent and identically distributed (i.i.d) over the blocks b and across antennas q, with zero mean and variance σ_X^2 and σ_H^2 per dimension, respectively. As a result, the received signal $Z_{qb}(k)$ is also i.i.d with zero mean and variance $\sigma_Z^2 = 2\sigma_H^2\sigma_X^2$ per dimension. The noise $W_{qb}(k)$ is assumed to be a complex Gaussian processes with zero mean and variance σ_W^2 per dimension, i.e. $W_{qb}(k) \sim \mathcal{CN}_{(0,2\sigma_W^2)}$.

Lemma 1: When the primary system is not transmitting, $|\lambda(i)|$ has a Rayleigh distribution for all i, i.e. the following cumulative density function (CDF) and mean:

$$\mathrm{P}_\lambda(|\lambda(i)| \le R) = 1 - \exp\big(-\frac{R^2}{16\sigma_W^8/N}\big) \tag{12}$$

$$\mathrm{E}\big\{|\lambda(i)|\big\} = 2\sigma_W^4\sqrt{\frac{\pi}{N}} \tag{13}$$

Lemma 2: When the primary system is transmitting, $|\lambda(i)|$ has a Rayleigh distribution with the following mean:

$$\mathrm{E}\big\{|\lambda(i)|\big\} = \sqrt{\frac{\pi}{2N}}\big(8\sigma_Z^8 + 32\sigma_Z^6\sigma_W^2 + 48\sigma_Z^4\sigma_W^4 + 32\sigma_Z^2\sigma_W^6 + 8\sigma_W^8\big)^{\frac{1}{2}} \qquad \forall i \neq 0 \tag{14}$$

whereas $|\lambda(0)|$ is approximated by a Rician distribution with the following parameters:

$$\mathrm{E}\big\{\lambda(0)\big\} = 4\sigma_Z^4 \tag{15}$$

and variance per dimension:

$$\begin{aligned}\mathrm{Var}\big\{\mathrm{Re}\big\{\lambda(0)\big\}\big\} &\approx \mathrm{Var}\big\{\mathrm{Im}\big\{\lambda(0)\big\}\big\} \\ &\approx \frac{\big(48\sigma_Z^4\sigma_W^4 + 32\sigma_Z^2\sigma_W^6 + 8\sigma_W^8\big)}{N}\end{aligned} \tag{16}$$

The proofs of these lemmas are based on the central limit theorem and are given in the Appendix. From Eq. (11), (12) and (13), we can derive the probability of false alarm:

$$\begin{aligned}\mathrm{P_{fa}} &= \mathrm{P}\big(T_1/T_2 > \gamma \mid \mathcal{H}_0\big) = \mathrm{P}\big(|\lambda(0)| > \gamma\mathrm{E}\big\{|\lambda(i)|\big\} \mid \mathcal{H}_0\big) \\ &= 1 - \mathrm{P}_\lambda\big(|\lambda(0)| \le \gamma\mathrm{E}\big\{|\lambda(i)|\big\}\big) \\ &= \exp\big(-\frac{\gamma^2\pi}{4}\big)\end{aligned} \tag{17}$$

Eq. (17) indicates that the $\mathrm{P_{fa}}$ does not depend on the noise variance nor the block size N. It is a function of the threshold value only. For a target $\mathrm{P_{fa}}$, we can use the following threshold:

$$\gamma = \sqrt{-\frac{4\log_e(P_{fa})}{\pi}} \tag{18}$$

Furthermore, based on Lemma 2, the probability of detection is derived as:

$$\begin{aligned}\mathrm{P_d} &= \mathrm{P}\big(T_1/T_2 > \gamma \mid \mathcal{H}_1\big) = \mathrm{P}\big(\mathrm{E}\big\{|\lambda(0)|\big\} > \gamma\mathrm{E}\big\{|\lambda(i)|\big\} \mid \mathcal{H}_1\big) \\ &\approx \mathrm{Q}_1\Big(\frac{4\mathrm{SNR}^2}{\sqrt{\frac{1}{N}\big(48\mathrm{SNR}^2 + 32\mathrm{SNR} + 8\big)}}, \\ &\quad \frac{\gamma\sqrt{\frac{\pi}{2N}\big(8\mathrm{SNR}^4 + 32\mathrm{SNR}^3 + 48\mathrm{SNR}^2 + 32\mathrm{SNR} + 8\big)}}{\sqrt{\frac{1}{N}\big(48\mathrm{SNR}^2 + 32\mathrm{SNR} + 8\big)}}\Big)\end{aligned} \tag{19}$$

where $\mathrm{Q}_1(a,b)$ is the Marcum Q-function of the first order [11], and $\mathrm{SNR} \triangleq \frac{\sigma_Z^2}{\sigma_W^2}$ is the energy per symbol per noise power spectral density.

A. Computational complexity

The algorithm requires two FFT operations per receive antenna, each costs $O(N\log_2 N)$ operations. The circular correlation implemented via FFT requires $O(N\log_2 N)$. In total, the algorithm's complexity is $O(\mathcal{Q}N\log_2 N)$. For comparison, the eigenvalue-based Blindly Combining Energy Detection (BCED) method requires about $O(\mathcal{Q}NL + \mathcal{Q}^3L^3)$, where L is the smoothing factor [9]. When $\log_2 N < L$, our algorithm's complexity is lower than that of existing methods.

IV. Numerical Results

In this section, we evaluate the performance of the proposed scheme by Monte Carlo simulations. The main system parameters used in simulations are summarized in Table I. The performance of the proposed scheme is compared with those of the BCED, and for fair comparison, the BCED also works on two blocks per antenna, such that the total number of samples is $N_s = 2N$.

TABLE I
SIMULATION PARAMETERS

Parameter	Value
Primary transmitter	
System modulation	Orthogonal Frequency-Division Multiplexing
System bandwidth	40MHz
Number of subcarriers	1024
Cyclic prefix	300
Subcarrier modulation	Binary Phase Shift Keying
Number of Tx antennas	1
Propagation channel	
Channel model	7-tap exponential decay Rayleigh fading [12]
Channel delay spread	$1\mu s$
Secondary receiver	
Number of Rx antennas	2

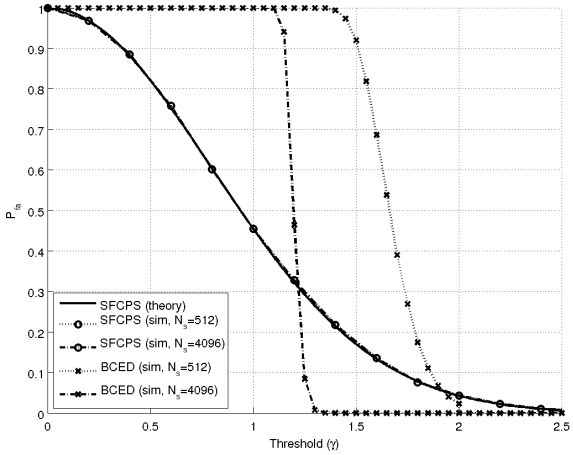

Fig. 2. The choice of threshold based on the target probability of false alarm

Figure 2 shows the dependency of $\mathrm{P_{fa}}$ on the threshold value and it validates our analysis in Section III. $\mathrm{P_{fa}}$ in SFCPS is a function of the threshold only, representing a significant adavantage compared to BCED. $\mathrm{P_{fa}}$ of BCED varies with N_s: as N_s increases, the variation becomes more abrupt, which means a small error in threshold level could introduce large error in the outcome $\mathrm{P_{fa}}$.

We set the target $\mathrm{P_{fa}} = 10\%$ and vary the SNR to obtain the corresponding probability of detection in Figure 3. Since the $\mathrm{P_d}$ of the BCED scheme depends on large N_s to compensate for weak correlation strength among receive signal samples [9], we can observe the *ceiling effect*: the $\mathrm{P_d}$ does not converge to 1 for small N_s, irrespective of how high the SNR is. The SFCPS scheme outperforms the BCED especially for a small number of samples N_s, and it can reach 100% probability of detect when the SNR allows. The theoretical analysis is proven to be a close approximation of the actual $\mathrm{P_d}$ performance, especially at low SNR region.

V. CONCLUSIONS

This paper proposes a frequency domain spectrum sensing method applicable to frequency selective channels and receivers equipped with two antennas. Extensive analysis has been accomplished to give its theoretical performance in terms

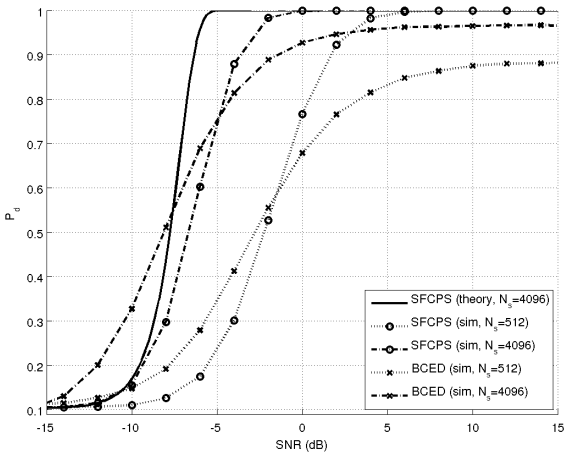

Fig. 3. $\mathrm{P_d}$ versus SNR for OFDM signal at $\mathrm{P_{fa}} = 10\%$

of both probability of false alarm and probability of detection. From analysis and numerical evaluations, the proposed method is shown to have high performance without using the knowledge about the signal, channel and noise power. It outperforms the reference scheme with a small number of samples and with a lower complexity. This technique can be extended to secondary devices with more than 2 antennas, which is the object of future research.

APPENDIX
PROOF OF LEMMAS

The hypothesis testing problem based on two blocks of N samples over two receive antennas are as follows:

$$\mathcal{H}_0 : \begin{cases} \mathbf{Y}_{11} \odot \mathbf{Y}_{22} &= \mathbf{W}_{11} \odot \mathbf{W}_{22} \\ \mathbf{Y}_{12} \odot \mathbf{Y}_{21} &= \mathbf{W}_{12} \odot \mathbf{W}_{21} \end{cases} \tag{20}$$

$$\mathcal{H}_1 : \begin{cases} \mathbf{Y}_{11} \odot \mathbf{Y}_{22} &= \mathbf{Z}_{11} \odot \mathbf{Z}_{22} + \mathbf{Z}_{11} \odot \mathbf{W}_{22} + \\ & \quad \mathbf{Z}_{22} \odot \mathbf{W}_{11} + \mathbf{W}_{11} \odot \mathbf{W}_{22} \\ \mathbf{Y}_{12} \odot \mathbf{Y}_{21} &= \mathbf{Z}_{12} \odot \mathbf{Z}_{21} + \mathbf{Z}_{12} \odot \mathbf{W}_{21} + \\ & \quad \mathbf{Z}_{12} \odot \mathbf{W}_{21} + \mathbf{W}_{12} \odot \mathbf{W}_{22} \end{cases}$$

For notation simplicity, we define $\mathbf{V}_{1i} \triangleq \mathrm{cshift}\big(\mathbf{Y}_{11} \odot \mathbf{Y}_{22}, i\big)$, $\mathbf{V}_{2i} \triangleq \mathrm{cshift}\big(\mathbf{Y}_{12} \odot \mathbf{Y}_{21}, i\big)$. We notice that Eq. (10) can be simply written as: $\lambda(i) = \frac{1}{N}\mathbf{V}_{10}^H \mathbf{V}_{2i}$. Likewise, we define: $\mathbf{A}_{1i} \triangleq \mathrm{cshift}\big(\mathbf{Z}_{11} \odot \mathbf{Z}_{22}, i\big)$, $\mathbf{A}_{2i} \triangleq \mathrm{cshift}\big(\mathbf{Z}_{12} \odot \mathbf{Z}_{21}, i\big)$, $\mathbf{B}_{1i} \triangleq \mathrm{cshift}\big(\mathbf{Z}_{11} \odot \mathbf{W}_{22}, i\big)$, $\mathbf{B}_{2i} \triangleq \mathrm{cshift}\big(\mathbf{Z}_{12} \odot \mathbf{W}_{21}, i\big)$, $\mathbf{C}_{1i} \triangleq \mathrm{cshift}\big(\mathbf{Z}_{22} \odot \mathbf{W}_{11}, i\big)$, $\mathbf{C}_{2i} \triangleq \mathrm{cshift}\big(\mathbf{Z}_{12} \odot \mathbf{W}_{21}, i\big)$, $\mathbf{D}_{1i} \triangleq \mathrm{cshift}\big(\mathbf{W}_{11} \odot \mathbf{W}_{22}, i\big)$ and $\mathbf{D}_{2i} \triangleq \mathrm{cshift}\big(\mathbf{W}_{12} \odot \mathbf{W}_{21}, i\big)$, where $\mathrm{cshift}\big(\mathbf{x}, i\big)$ indicates the circular shift of vector $\mathbf{x}$ by i elements to the right.

Proof of Lemma 1: Replacing the null hypothesis of Eq. (20) into (10), we have:

$$\lambda(i) = \frac{1}{N}\mathbf{D}_{10}^H \mathbf{D}_{2i} = \frac{1}{N}\big(\mathbf{D}_{I10}^T \mathbf{D}_{I2i} + \mathbf{D}_{Q10}^T \mathbf{D}_{Q2i}\big) + j\frac{1}{N}\big(\mathbf{D}_{I10}^T \mathbf{D}_{Q2i} - \mathbf{D}_{Q10}^T \mathbf{D}_{I2i}\big) \tag{21}$$

where $\mathbf{D}_{Ivi} \triangleq [W_{vi}^I(0)\ W_{vi}^I(1) \ldots\ W_{vi}^I(N-1)]^T$ and $\mathbf{D}_{Qvi} \triangleq [W_{vi}^Q(0)\ W_{vi}^Q(1) \ldots\ W_{vi}^Q(N-1)]^T$ denotes the real

and imaginary part of $\mathbf{D}_{vi}$ $(v = 1, 2)$, respectively. Without loss of generality, we analyze only the first term in Eq. (21):

$$\begin{aligned}
&\frac{1}{N}\mathbf{D}_{I10}^T\mathbf{D}_{I2i} = \\
&\frac{1}{N}\sum_{k=0}^{N-1}\big[W_{11}^I(k)W_{22}^I(k)W_{12}^I(\lfloor k-i\rfloor_N)W_{21}^I(\lfloor k-i\rfloor_N) \\
&- W_{11}^Q(k)W_{22}^Q(k)W_{12}^I(\lfloor k-i\rfloor_N)W_{21}^I(\lfloor k-i\rfloor_N) \\
&- W_{11}^I(k)W_{22}^I(k)W_{12}^Q(\lfloor k-i\rfloor_N)W_{21}^Q(\lfloor k-i\rfloor_N) \\
&+ W_{11}^Q(k)W_{22}^Q(k)W_{12}^Q(\lfloor k-i\rfloor_N)W_{21}^Q(\lfloor k-i\rfloor_N)\big] \qquad (22)
\end{aligned}$$

For large N, based on the central limit theorem, we can show that this term has normal distribution, i.e. $\mathbf{D}_{I10}^T\mathbf{D}_{I2i} \sim \mathcal{N}_{(0,\frac{4}{N}\sigma_W^8)}$. The same goes true for other terms in Eq. (21), and therefore $\lambda(i) \sim \mathcal{CN}_{(0,\frac{16}{N}\sigma_W^8)}$. As a result, the envelop of $\lambda(i)$ has Rayleigh distributed with the CDF and mean given in Eq. (12) and (13), respectively [13]. ■

Proof of Lemma 2: Put the alternative hypothesis of Eq. (20) into (10), we have:

$$\begin{aligned}
\lambda(i) = \frac{1}{N}\big(&\mathbf{A}_{10}^H\mathbf{A}_{2i} + \mathbf{A}_{10}^H\mathbf{B}_{2i} + \mathbf{A}_{10}^H\mathbf{C}_{2i} + \mathbf{A}_{10}^H\mathbf{D}_{2i} \\
&+ \mathbf{B}_{10}^H\mathbf{A}_{2i} + \mathbf{B}_{10}^H\mathbf{B}_{2i} + \mathbf{B}_{10}^H\mathbf{C}_{2i} + \mathbf{B}_{10}^H\mathbf{D}_{2i} \\
&+ \mathbf{C}_{10}^H\mathbf{A}_{2i} + \mathbf{C}_{10}^H\mathbf{B}_{2i} + \mathbf{C}_{10}^H\mathbf{C}_{2i} + \mathbf{C}_{10}^H\mathbf{D}_{2i} \\
&+ \mathbf{D}_{10}^H\mathbf{A}_{2i} + \mathbf{D}_{10}^H\mathbf{B}_{2i} + \mathbf{D}_{10}^H\mathbf{C}_{2i} + \mathbf{D}_{10}^H\mathbf{D}_{2i}\big) \qquad (23)
\end{aligned}$$

Case $i \neq 0$: Using a similar proof as in Lemma 1, where the central limit theorem is applied, we can show that each term in Eq. (23) is complex normal distributed, specifically $\mathbf{A}_{10}^H\mathbf{A}_{2i} \sim \mathcal{CN}_{(0,\frac{16}{N}\sigma_Z^8)}$, $\mathbf{A}_{10}^H\mathbf{B}_{2i} \sim \mathcal{CN}_{(0,\frac{16}{N}\sigma_Z^6\sigma_W^2)}$, $\mathbf{A}_{10}^H\mathbf{C}_{2i} \sim \mathcal{CN}_{(0,\frac{16}{N}\sigma_Z^6\sigma_W^2)}$, $\mathbf{A}_{10}^H\mathbf{D}_{2i} \sim \mathcal{CN}_{(0,\frac{16}{N}\sigma_Z^4\sigma_W^4)}$, $\mathbf{B}_{10}^H\mathbf{A}_{2i} \sim \mathcal{CN}_{(0,\frac{16}{N}\sigma_Z^6\sigma_W^2)}$, $\mathbf{B}_{10}^H\mathbf{B}_{2i} \sim \mathcal{CN}_{(0,\frac{16}{N}\sigma_Z^4\sigma_W^4)}$, $\mathbf{B}_{10}^H\mathbf{C}_{2i} \sim \mathcal{CN}_{(0,\frac{16}{N}\sigma_Z^4\sigma_W^4)}$, $\mathbf{B}_{10}^H\mathbf{D}_{2i} \sim \mathcal{CN}_{(0,\frac{16}{N}\sigma_Z^2\sigma_W^6)}$, $\mathbf{C}_{10}^H\mathbf{A}_{2i} \sim \mathcal{CN}_{(0,\frac{16}{N}\sigma_Z^6\sigma_W^2)}$, $\mathbf{C}_{10}^H\mathbf{B}_{2i} \sim \mathcal{CN}_{(0,\frac{16}{N}\sigma_Z^4\sigma_W^4)}$, $\mathbf{C}_{10}^H\mathbf{C}_{2i} \sim \mathcal{CN}_{(0,\frac{16}{N}\sigma_Z^4\sigma_W^4)}$, $\mathbf{C}_{10}^H\mathbf{D}_{2i} \sim \mathcal{CN}_{(0,\frac{16}{N}\sigma_Z^2\sigma_W^6)}$, $\mathbf{D}_{10}^H\mathbf{A}_{2i} \sim \mathcal{CN}_{(0,\frac{16}{N}\sigma_Z^4\sigma_W^4)}$, $\mathbf{D}_{10}^H\mathbf{B}_{2i} \sim \mathcal{CN}_{(0,\frac{16}{N}\sigma_Z^2\sigma_W^6)}$, $\mathbf{D}_{10}^H\mathbf{C}_{2i} \sim \mathcal{CN}_{(0,\frac{16}{N}\sigma_Z^2\sigma_W^6)}$ and $\mathbf{D}_{10}^H\mathbf{D}_{2i} \sim \mathcal{CN}_{(0,\frac{16}{N}\sigma_W^8)}$. Therefore, $\lambda(i)$ is also zero-mean complex normal distributed, i.e. $\lambda(i) \sim \mathcal{CN}_{(0,\frac{16}{N}(\sigma_Z^8+4\sigma_Z^6\sigma_W^2+6\sigma_Z^4\sigma_W^4+4\sigma_Z^2\sigma_W^6+\sigma_W^8))}$. Hence, $|\lambda(i)|$ has Rayleigh distribution with the mean given in Eq. (14) [13].

Case $i = 0$: From Eq. (8), we have $\mathbf{A}_{10} = \mathbf{A}_{20}$ and Eq. (23) becomes:

$$\begin{aligned}
\lambda(0) = \frac{1}{N}\big(&\mathbf{A}_{10}^H\mathbf{A}_{10} + \mathbf{A}_{10}^H\mathbf{B}_{20} + \mathbf{A}_{10}^H\mathbf{C}_{20} + \mathbf{A}_{10}^H\mathbf{D}_{20} \\
&+ \mathbf{B}_{10}^H\mathbf{A}_{10} + \mathbf{B}_{10}^H\mathbf{B}_{20} + \mathbf{B}_{10}^H\mathbf{C}_{20} + \mathbf{B}_{10}^H\mathbf{D}_{20} \\
&+ \mathbf{C}_{10}^H\mathbf{A}_{10} + \mathbf{C}_{10}^H\mathbf{B}_{20} + \mathbf{C}_{10}^H\mathbf{C}_{20} + \mathbf{C}_{10}^H\mathbf{D}_{20} \\
&+ \mathbf{D}_{10}^H\mathbf{A}_{10} + \mathbf{D}_{10}^H\mathbf{B}_{20} + \mathbf{D}_{10}^H\mathbf{C}_{20} + \mathbf{D}_{10}^H\mathbf{D}_{20}\big) \qquad (24)
\end{aligned}$$

Similarly, after tedious but straightforward derivation, we can show that the first term in Eq. (24) is real and normal distributed, i.e. $\mathbf{A}_{10}^H\mathbf{A}_{10} \sim \mathcal{N}_{(4\sigma_Z^4,\frac{4}{N}(\beta_Z^2-\sigma_Z^8))}$, while the other terms are complex normal distributed, namely $\mathbf{A}_{10}^H\mathbf{B}_{20} \sim \mathcal{CN}_{(0,\frac{16}{N}\beta_Z\sigma_Z^2\sigma_W^2)}$, $\mathbf{A}_{10}^H\mathbf{C}_{20} \sim \mathcal{CN}_{(0,\frac{16}{N}\beta_Z\sigma_Z^2\sigma_W^2)}$, $\mathbf{A}_{10}^H\mathbf{D}_{20} \sim \mathcal{CN}_{(0,\frac{16}{N}\sigma_Z^4\sigma_W^4)}$, $\mathbf{B}_{10}^H\mathbf{A}_{10} \sim \mathcal{CN}_{(0,\frac{16}{N}\beta_Z\sigma_Z^2\sigma_W^2)}$, $\mathbf{B}_{10}^H\mathbf{B}_{20} \sim \mathcal{CN}_{(0,\frac{16}{N}\sigma_Z^4\sigma_W^4)}$, $\mathbf{B}_{10}^H\mathbf{C}_{20} \sim \mathcal{CN}_{(0,\frac{16}{N}\sigma_Z^4\sigma_W^4)}$, $\mathbf{B}_{10}^H\mathbf{D}_{20} \sim \mathcal{CN}_{(0,\frac{16}{N}\sigma_Z^2\sigma_W^6)}$, $\mathbf{C}_{10}^H\mathbf{A}_{10} \sim \mathcal{CN}_{(0,\frac{16}{N}\beta_Z\sigma_Z^2\sigma_W^2)}$, $\mathbf{C}_{10}^H\mathbf{B}_{20} \sim \mathcal{CN}_{(0,\frac{16}{N}\sigma_Z^4\sigma_W^4)}$, $\mathbf{C}_{10}^H\mathbf{C}_{20} \sim \mathcal{CN}_{(0,\frac{16}{N}\sigma_Z^4\sigma_W^4)}$, $\mathbf{C}_{10}^H\mathbf{D}_{20} \sim \mathcal{CN}_{(0,\frac{16}{N}\sigma_Z^2\sigma_W^6)}$, $\mathbf{D}_{10}^H\mathbf{A}_{10} \sim \mathcal{CN}_{(0,\frac{16}{N}\sigma_Z^4\sigma_W^4)}$, $\mathbf{D}_{10}^H\mathbf{B}_{20} \sim \mathcal{CN}_{(0,\frac{16}{N}\sigma_Z^2\sigma_W^6)}$, $\mathbf{D}_{10}^H\mathbf{C}_{20} \sim \mathcal{CN}_{(0,\frac{16}{N}\sigma_Z^2\sigma_W^6)}$ and $\mathbf{D}_{10}^H\mathbf{D}_{20} \sim \mathcal{CN}_{(0,\frac{16}{N}\sigma_W^8)}$ where β_Z is the forth moment of the real (or imaginary) part of $Z_{qb}(k)$. As a result, $\lambda(0) \sim \mathcal{N}_{(4\sigma_Z^4,\frac{(4\beta_Z^2-4\sigma_Z^8+32\beta_Z\sigma_Z^2\sigma_W^2+48\sigma_Z^4\sigma_W^4+32\sigma_Z^2\sigma_W^6+8\sigma_W^8)}{N})} + j\mathcal{N}_{(0,\frac{32\beta_Z\sigma_Z^2\sigma_W^2+48\sigma_Z^4\sigma_W^4+32\sigma_Z^2\sigma_W^6+8\sigma_W^8}{N})}$.

The fourth moment β_Z is tricky to derive, and it might not have a closed form expression. Therefore we consider the following approximation: if the SNR is low, i.e. the noise variance is more dominant than the signal variance, we can neglect the following terms β_Z^2, $\beta_Z\sigma_Z^2\sigma_W^2$ σ_Z^8, $\sigma_Z^6\sigma_W^2$. Thus:

$$\lambda(0) \sim \mathcal{CN}_{(4\sigma_Z^4,\frac{96\sigma_Z^4\sigma_W^4+64\sigma_Z^2\sigma_Z^6\sigma_W^6+16\sigma_W^8}{N})} \qquad (25)$$

It is well-known that the envelop of $\lambda(0)$ has Rician distribution with parameters given in Eq. (14) and (16) [13]. ■

ACKNOWLEDGEMENT

The authors would like to thank the Center for TeleInFrastrucktur (CTIF), Aalborg University, Denmark and the National Institute of Information and Communications (NICT), Japan for supporting this work.

REFERENCES

[1] Y. Zeng, Y.-C. Liang, A. T. Hoang, and Y.-C. Liang, "A Review on Spectrum Sensing for Cognitive Radio: Challengs and Solutions," *EURASIP Journal on Advances in Signal Processing*, 2010.

[2] S. M. Kay, *Fundamentals of Statistical Signal Processing: Detection Theory*. Prentice Hall, 1998, vol. 2.

[3] N. Han, S. Shon, J. H. Chung, and J. M. Kim, "Spectral correlation based signal detection method for spectrum sensing in ieee 802.22 wran systems," in *Advanced Communication Technology, 2006. ICACT 2006. The 8th International Conference*, vol. 3, February 2006, pp. 6 pp. – 1770.

[4] H. Urkowitz, "Energy detection of unknown deterministic signals," *Proceedings of the IEEE*, vol. 55, no. 4, pp. 523 – 531, April 1967.

[5] F. F. Digham, M.-S. Alouini, and M. K. Simon, "On the energy detection of unknown signals over fading channels," *Communications, IEEE Transactions on*, vol. 55, no. 1, pp. 21 –24, January 2007.

[6] Z. Tian and G. B. Giannakis, "A wavelet approach to wideband spectrum sensing for cognitive radios," in *Cognitive Radio Oriented Wireless Networks and Communications, 2006. 1st International Conference on*, June 2006, pp. 1 –5.

[7] Y. Zeng and Y.-C. Liang, "Spectrum-Sensing Algorithms for Cognitive Radio Based on Statistical Covariances," *IEEE Transactions on Vehicular Technology*, May 2009.

[8] Y. Zeng, Y.-C. Liang, and R. Zhang, "Blindly combined energy detection for spectrum sensing in cognitive radio," *Signal Processing Letters, IEEE*, vol. 15, pp. 649 –652, 2008.

[9] Y. Zeng and Y.-C. Liang, "Eigenvalue-based spectrum sensing algorithms for cognitive radio," *Communications, IEEE Transactions on*, vol. 57, no. 6, pp. 1784 –1793, June 2009.

[10] J. G. Proakis and D. G. Manolakis, *Digital Signal Processing: Principles, Algorithms and Applications*, 4th ed. Prentice Hall, August 2006.

[11] P. Y. Kam and R. Li, "Computing and bounding the first-order marcum q-function: a geometric approach," *Communications, IEEE Transactions on*, vol. 56, no. 7, pp. 1101 –1110, 2008.

[12] R. Vaughan and J. B. Andersen, *Channels propagation and antennas for mobile communications*. IEE Electromagnetic Waves Series 50, 2003, no. ISBN 0-85296084-0.

[13] J. D. Parsons, *The Mobile Radio Propagation Channel, 2nd Edition*, 2nd ed. Wiley Europe, November 2000.